

## Evaluation of an Improved Convective Triggering Function: Observational Evidence and SCM Tests

Yi-Chi Wang<sup>1</sup> , Shaocheng Xie<sup>2</sup> , Shuaiqi Tang<sup>2</sup> , and Wuyin Lin<sup>3</sup><sup>1</sup>Research Center for Environmental Changes, Academia Sinica, Taipei, Taiwan, <sup>2</sup>Lawrence Livermore National Laboratory, Livermore, CA, USA, <sup>3</sup>Brookhaven National Laboratory, Upton, NY, USA**Key Points:**

- A dynamic CAPE (dCAPE) trigger combined with an unrestricted air parcel launch level (ULL) is strongly supported by the ARM observations
- The dCAPE trigger suppresses spurious daytime convection more effectively under tropical environment than midlatitude environment
- ULL plays a bigger role in improving rainfall diurnal cycle by catching nocturnal elevated convection and suppressing morning convection

**Correspondence to:**Shaocheng Xie,  
xie2@llnl.gov**Citation:**Wang, Y.-C., Xie, S., Tang, S., & Lin, W. (2020). Evaluation of an improved convective triggering function: Observational evidence and SCM tests. *Journal of Geophysical Research: Atmospheres*, 125, e2019JD031651. <https://doi.org/10.1029/2019JD031651>

Received 23 SEP 2019

Accepted 21 APR 2020

Accepted article online 23 APR 2020

**Abstract** This study provides a strong observational support for a recently developed convective triggering function that uses the large-scale dynamic convective available potential energy (dCAPE) as a constraint combined with an unrestricted air parcel launch level (ULL) to relax the unrealistic strong coupling of convection to surface heating and capture nocturnal elevated convection. Both case study and statistical analysis are conducted using the observations collected from the Department of Energy's Atmospheric Radiation Measurement program at its Southern Great Plains and Manaus (MAO) sites. They show that dCAPE has a much stronger correlation with precipitation than convective available potential energy, and ULL is essential to detect elevated convection above boundary layer under both midlatitude and tropical conditions and for both afternoon and nighttime deep convection regimes. Sensitivity tests with the single-column model (SCM) of the Department of Energy's Energy Exascale Earth System Model indicate that the role of dCAPE in suppressing daytime convection is more effective for tropical convection than midlatitude convection. Even though the dCAPE can suppress the overestimated convection, ULL plays a much bigger role in improving the diurnal cycle of precipitation than dCAPE. It not only helps capture nocturnal elevated convection but also significantly removes the spurious morning precipitation seen in the default model, due to the release of unstable energy at night. However, the use of ULL has led to an overestimation of light-to-moderate precipitation (1–10 mm/day) due to more convection being triggered above boundary layer.

### 1. Introduction

Convective trigger is a key part of cumulus parameterizations used in weather and climate models. It determines when and where model convection will occur and thus affects the precipitation variability and distributions. In general, model convection is triggered when convective instability in the atmospheric vertical column, that is, the presence of significant positive convective available potential energy (CAPE), is detected. However, this type of trigger results in an unrealistically strong coupling of convection to the surface heating, which is largely controlled by solar insolation in summer (Lee et al., 2007; Xie & Zhang, 2000). As a result, model convection is triggered too easily during the day particularly over land in summer. This also partially causes the failure of capturing nocturnal convection in many models (Lee et al., 2007, 2008; Surcel et al., 2010; Zheng et al., 2019) since nocturnal convection is often elevated and decoupled from the surface (Geerts et al., 2017; Marsham et al., 2011; Xie et al., 2014).

To reduce the strong surface control on model convection initiation and prevent CAPE from being released spontaneously, many studies attempted to link convective trigger to the large-scale dynamic processes such as the large-scale advection of temperature and moisture and low-level convergence since these processes play a key role in destabilizing the atmospheric structure and initiating moist convection. For example, the Kain-Fritsch scheme (Fritsch & Chappell, 1980; Kain, 2004; Kain & Fritsch, 1992) included the effect of perturbed temperature and vertical velocity from the environmental upward motion on convection onset within large-scale ascending region. Bechtold et al. (2014) considered the coupling with low-level moisture in estimating the available energy in its convective triggering function and suggested convection being favored in the moist environment. Xie and Zhang (2000) found that convection is often triggered when the large-scale dynamics make a positive contribution to the existing CAPE based on field observations. They proposed to use the dynamical CAPE (dCAPE), which is the measure of the CAPE generation rate due to the large-scale dynamics, as a convective trigger mechanism. The strong

correlation between positive dCAPE and precipitation was also found in J. Wang and Randall (1994) and Randall and Wang (1991). Application of the dCAPE trigger in a climate model has shown significant improvements in the precipitation patterns over both the Contiguous United States and around the globe (Xie, Cederwall, & Zhang, 2004). Suhas and Zhang (2014) and Song and Zhang (2017) tested several commonly used convective triggering mechanisms against the data collected from the Department of Energy's Atmospheric Radiation Measurement program (ARM) and found that the dCAPE trigger has the best performance in capturing convection initiation. Sakaguchi et al. (2018) applied the dCAPE trigger to the Community Atmospheric Model version 5 (CAM5) that resulted in an improvement in both nocturnal and late afternoon precipitation amount over the Amazon region.

However, the dCAPE trigger and most other commonly used triggers may not work well for summertime nocturnal convection observed in some regions such as the Southern Great Plains (SGP), where most nocturnal precipitating events are associated with the propagation of mesoscale convective systems (MCSs) and are elevated above the stable boundary layer (Geerts et al., 2017). Under such condition, no instability could be detected for a parcel lifting from near-surface levels as is often the case effectively in some convection schemes such as the G. J. Zhang and Mcfarlane (1995) scheme (ZM, hereafter). To capture the elevated nocturnal convective systems, removing the constraint of air parcel launch level within boundary layer is necessary as demonstrated in Han and Pan (2011) and Y. C. Wang et al. (2015). Here, we call this method as the unrestricted air parcel launch level (ULL) trigger.

Motivated by these earlier studies, Xie et al. (2019) proposed a new triggering mechanism by combining the dCAPE trigger and the ULL trigger to improve climate models in capturing convection initiation, particularly to address current model issues in capturing the diurnal cycle of precipitation. For convenience, we call the trigger as dCAPE&ULL. The philosophy of dCAPE&ULL is that the dCAPE trigger provides a dynamic constraint for preconditioning of convection-favored environment to establish and preventing CAPE from being released spontaneously during the day when CAPE is often generated due to solar heating at surface, therefore making CAPE available for nocturnal convective activities. Meanwhile, the ULL trigger removes the constraint that convection always has its root near the surface and therefore allows elevated convection to be captured. Xie et al. (2019) has shown that the dCAPE&ULL trigger significantly improves the diurnal cycle of precipitation simulated by the Department of Energy's newly developed Energy Exascale Earth System Model (E3SM) atmosphere model version 1 (EAMv1) (Golaz et al., 2019; Rasch et al., 2019; Xie et al., 2018), which uses ZM as the deep cumulus scheme, in an 11-year Atmospheric Model Intercomparison Project (AMIP)-style climatology run.

In this paper, we evaluate the dCAPE&ULL trigger using detailed ARM observations collected in different climate regimes. The single-column model (SCM) version of the E3SM (<https://github.com/E3SM-Project/scmlib/wiki/E3SM-Single-Column-Model-Home>) is also used to test the new trigger under a situation that the large-scale forcing is specified from the ARM observations. The goal is to examine how well the underlying physical mechanisms of dCAPE&ULL are supported by the observations and what relative roles dCAPE and ULL play in simulating the diurnal cycle of precipitation in various deep convection regimes under the SCM framework.

This paper is organized as follows. Section 2 provides more details on the dCAPE&ULL trigger. The observational data sets are described in section 3. Section 4 performs detailed observational analysis to examine the physics behind the dCAPE&ULL trigger. Section 5 utilizes the SCM framework to test its performance in capturing convective systems observed over different deep convection regimes. Section 6 summarizes the analysis and discusses its implications on future developments of convective triggers.

## 2. The dCAPE&ULL Trigger

As described in Xie et al. (2019), the dCAPE&ULL trigger includes two parts. The dCAPE trigger assumes that convection is initiated when the large-scale dynamic forcing makes a positive contribution to the existing CAPE. In another word, both CAPE and dCAPE need to be larger than zero for convection to be triggered. Here CAPE is defined as accumulated parcel buoyancy under the assumption that the air parcel ascends along the reversible moist adiabat.

$$CAPE = R_d \int_{P_i}^{P_n} (T_{vp} - T_v) d \ln p \quad (1)$$

where  $P_n$  is the equilibrium pressure level for the air parcel launching from  $P_i$ .  $T_{vp}$  is the virtual temperature for the launch parcel, while  $T_v$  is the environmental virtual temperature at the same vertical level.  $R_d$  is the gas constant of dry air.  $dCAPE$  is defined in Xie and Zhang (2000):

$$dCAPE = \frac{CAPE(T^*, q^*) - CAPE(T, q)}{\Delta t} \quad (2)$$

where  $(T, q)$  are the temperature and specific humidity of current environmental profile and  $(T^*, q^*)$  are the state for a hypothetical atmosphere, which are defined as  $(T, q)$  plus the changes due to the total large-scale dynamical advection over a time interval  $\Delta t$ , which is equal to the time step used in numerical models. To implement the  $dCAPE$  trigger in numerical models, we use the atmospheric states  $(T, q)$  saved before and after the dynamical core calculation at current time step for calculating  $dCAPE$ . In this way, we can ensure that the change of the atmospheric states is purely due to the large-scale advection. In an SCM framework, the advective tendencies can be specified from the observations.

The ULL trigger, described in Han and Pan (2011) and Y. C. Wang et al. (2015), works as the criterion for searching the source layer for launching air parcel used in the calculation of cloud properties and precipitation intensity. For example, in the ZM default scheme, the launching air parcel used for calculating the cloud top and associated CAPE is from the most unstable level of maximum moist static energy within the boundary layer. In contrast, the ULL trigger removes the boundary layer restriction by searching the source layer from surface up to 600 hPa. This criterion enables not only to capture surface-driven convection as the default ZM scheme does but also to capture source layer for elevated convection that decouples from the surface.

### 3. Observational Data

To validate the proposed triggering mechanisms, we utilize data collected from both Intensive Operational Periods (IOPs) and long-term multiyear continuous observations from the ARM SGP site and Manaus (MAO) site to cover convection over middle latitude and tropical lands for both case study and statistical analysis. The ARM SGP site (36.63°N, 97.49°W) is the first field measurement site established by ARM in the early 90s and offers the most extensive long-term observations of cloud, aerosol, and atmospheric processes for understanding cloud system over midlatitude land. At SGP, we use data collected from the Midlatitude Continental Convective Clouds Experiment (MC3E; Jensen et al., 2015) from 22 April to 6 June 2011 and the long-term multiyear periods that cover 12 summer seasons for years of 2004 to 2015.

The ARM MAO site (3.213°S, 60.598°W) was established for the Green Ocean Amazon (GoAmazon; Martin et al., 2016) field campaign from January 2014 to December 2015, aiming to document the cloud, precipitation, and aerosol variation for tropical forest regions around Manaus, Brazil. In this study we utilize its IOP1 data that cover the wet season from 15 February to 26 March 2014 for case study and the entire 2014–2015 2-year continuous observations for statistical analysis.

The large-scale advective tendencies and other geophysical quantities required to compute  $dCAPE$  and evaluate the new triggering mechanisms are from the ARM variational analysis (M. Zhang & Lin, 1997; M. Zhang et al., 2001). It uses surface and top of the atmosphere measurements of precipitation and radiative and turbulent fluxes to adjust background atmospheric state variables so that column-integrated mass, moisture, and energy budgets are closed. MC3E uses radiosonde combined with operational analysis as background fields (Xie, Zhang, et al., 2004), while the long-term forcing data at both SGP and MAO including the GoAmazon IOP1 data use only operational analysis/reanalysis as background fields (S. Tang et al., 2016; Xie, Zhang et al., 2004). Calculated from the adjusted atmospheric state variables, the large-scale advective tendencies and other variables are dynamically and thermodynamically consistent with the observed precipitation and fluxes. More information on how the variational analysis was applied to derive the large-scale advective forcing data products for MC3E, GoAmazon, and the ARM multiyear continuous forcing data at SGP can be seen in S. Tang et al. (2016), Xie et al. (2014), and Xie, Zhang, et al. (2004), respectively. Table 1 summarizes the data products used in this study.

**Table 1**  
*Summary of Observations*

Data source	Time period and location	References
MC3E IOP	22 April to 3 June 2011; SGP (USA)	Jensen et al. (2015) and Xie et al. (2014)
GoAmazon IOP1	15 February to 26 March 2014; MAO (Brazil)	Martin et al. (2016) and S. Tang et al. (2016)
SGP multiyear continuous observations	Summer months (JJA) for the period between 2004 and 2015; SGP (USA)	Xie, Zhang, et al. (2004) and Tang, Xie, et al. (2019)
GoAmazon	January 2014 to December 2015; MAO (Brazil)	Martin et al. (2016) and S. Tang et al. (2016)

## 4. Observational Evidence

### 4.1. Correlation Between CAPE/dCAPE With Precipitation

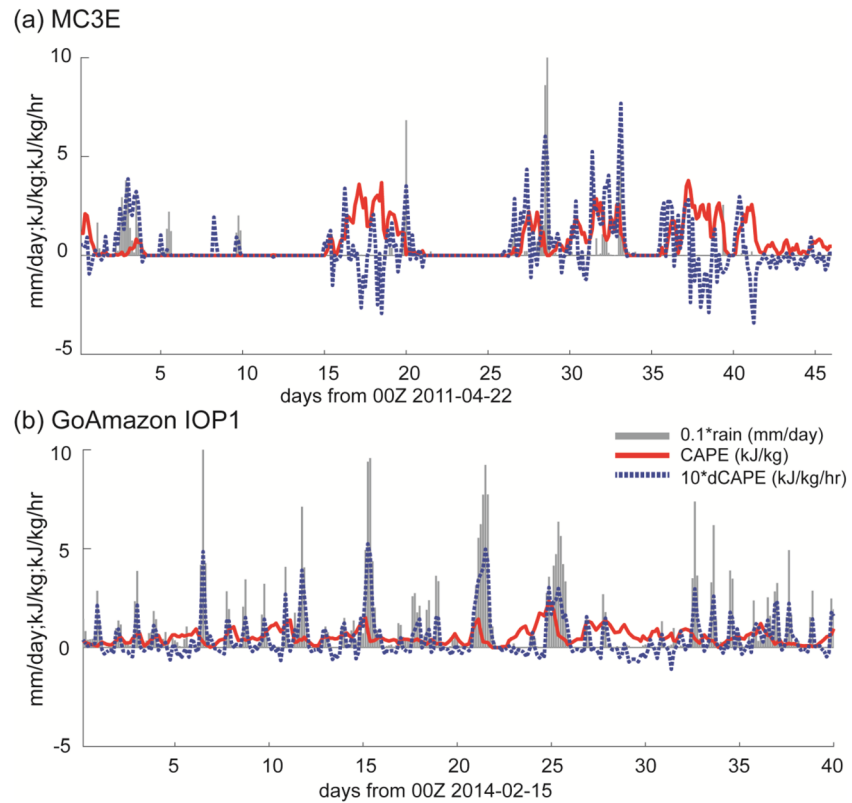
We first examine the correlation between CAPE/dCAPE and precipitation using the ARM IOP data and multiyear continuous measurements. Figure 1 shows the time series of CAPE, dCAPE, and precipitation for the MC3E and GoAmazon IOP1. Here CAPE is calculated under the assumption that an air parcel ascends along the reversible moist adiabat. The launch level is determined by the ULL method. It is clearly seen that CAPE has very distinct features among the two different convective regimes. For the midlatitude land convection case (MC3E), strong CAPE is often seen before strong convection events, indicating the accumulation of CAPE prior to convection. This feature is also seen in the tropical land convection case (GoAmazon), but CAPE is weaker with less variation. In addition, positive CAPE exists during almost entire field campaign regardless whether there is precipitation or not, suggesting the unstable nature of tropical atmosphere and potential issues with CAPE-based triggers. In contrast, convection correlates well with positive dCAPE that represents favorable convection environments in these two regimes. Furthermore, dCAPE also characterizes nonprecipitating periods with unfavorable environment conditions (i.e., negative dCAPE) in both regimes, such as the break period between convection events during the GoAmazon field campaign.

Figure 2 shows the scatter plots of dCAPE and CAPE with respect to precipitation intensity over SGP and MAO for both IOP periods, as well as the summer months June–July–August (JJA) for 2004–2015 for SGP and the entire 2-year period for MAO. For both regimes, dCAPE shows a positive correlation with precipitation intensity, while CAPE seems to be randomly distributed with respect to precipitation intensity. The correlation is more robust in the multiyear statistics as shown in Figures 2b and 2d compared to the IOP cases (Figures 2a and 2c). These results suggest that the positive dCAPE is well correlated with convection initiation and can even work as a closure to determine convection intensity as suggested in G. J. Zhang (2002, 2003). The result further indicates that dCAPE is a better indicator for convection onset and convection intensity than CAPE.

### 4.2. Role of ULL

Figure 3 investigates the impact of ULL on detecting convective instability by examining CAPE calculated for an air parcel launched from the surface and the level identified by ULL. As indicated in Figure 3b, which shows the difference between the ULL-based CAPE and the surface-based CAPE when convection occurs, the surface-based CAPE is smaller than the ULL-based CAPE for most of the time because the launched parcel is often of larger MSE from the level determined by ULL than the surface by definition. This is particularly true for nocturnal elevated convection cases where generally no CAPE is identified from an air parcel launched from the surface due to the strong stable boundary layer at night. This result suggests that model might underestimate convective precipitation, especially for the nocturnal convective events, when using the surface-based calculation for CAPE.

To further demonstrate how the proposed trigger works for nocturnal elevated convection, Figure 4 compares the CAPE and dCAPE calculated with launch level determined by the two methods for a selected nocturnal elevated convection event on 24–25 April 2014 in MC3E. As discussed in Xie et al. (2014), the



**Figure 1.** Time series of CAPE (kJ/kg) (red line) and dynamical CAPE (kJ/kg/hr) (blue dashed line) during the ARM field campaigns: (a) MC3E and (b) GoAmazon IOP1. The air parcel launch level is determined by ULL. The observed precipitation rate scaled by 10 (mm/day) is plotted as gray bars.

nocturnal elevated convection was decoupled from the surface with a very dry boundary layer. It is seen that both CAPE and dCAPE calculated from the surface are zero, indicating that they are not able to capture the convective instability above boundary layer, a common feature for nocturnal precipitation events over midlatitude land. In contrast, the elevated convection is well captured by using ULL.

### 4.3. Characteristics of CAPE/dCAPE on Afternoon and Nighttime Precipitation Days

The above discussion has indicated that positive dCAPE is a much better indicator than CAPE for convection onset, and ULL allows nocturnal elevated convection to be detected. In this subsection, we examine the characteristics of CAPE/dCAPE and the associated large-scale structures over different deep convection regimes to further understand how they would work as convective trigger under these conditions. Two regimes are selected for the analysis, afternoon (or early evening) deep convection regime and nighttime deep convection regime, using the multiyear ARM data at SGP and MAO. Following Y. Zhang and Klein (2010) with some modifications, an afternoon or early evening deep convection day is defined as (1) rain peak >1 mm/day, (2) peak time between 1300 and 2000 LST, and (3) peak rain rate >1.5 time of any rain rate outside of the period between 1300 and 2000 LST. The third condition is set to ensure the dominant mode of afternoon precipitation in the diurnal cycle. A nighttime deep convection day is defined as (1) rain peak >1 mm/day and (2) peak time between 0000 and 0700 LST. For SGP (MAO), there are a total of 99 (372) afternoon precipitation days and 290 (97) nighttime precipitation days.

Figure 5 shows the diurnal composite of precipitation and the associated large-scale forcing fields (i.e., total advective tendencies of dry static energy and moisture) over JJA at SGP for these two precipitation regimes. On afternoon deep convection days (Figures 5a and 5c), precipitation starts around local noon and peaks in late afternoon at 1700 LST with the maximum value around 10 mm/day, while on nighttime deep convection days (Figures 5b and 5d), precipitation starts around midnight and peaks at 0200–0300 LST with the peak value around 17 mm/day, suggesting that nighttime precipitation dominates the diurnal cycle of

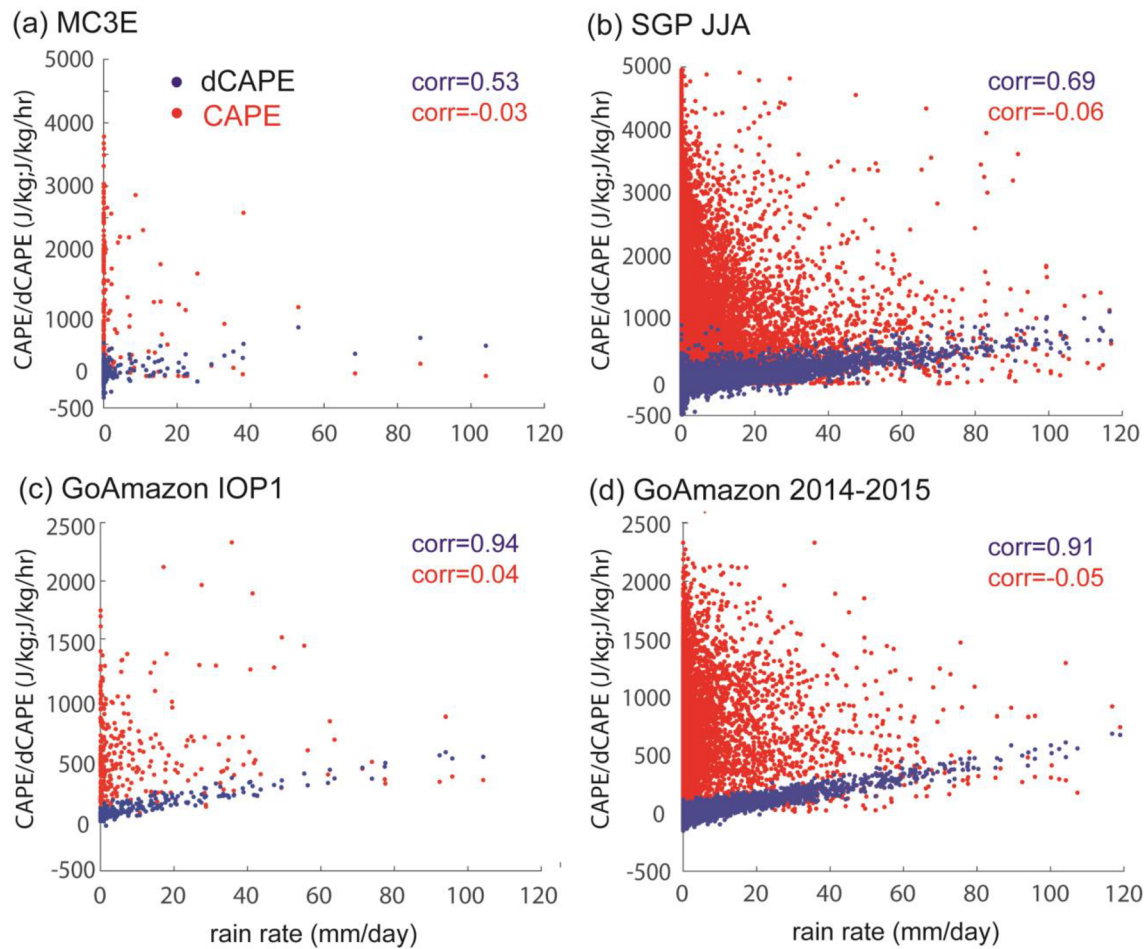


**Figure 2.** Scatter plots of CAPE and dCAPE with respect to precipitation intensity for both IOPs and long-term data sets: (a) MC3E, (b) SGP June–July–August (JJA) from 2004 to 2015, (c) GoAmazon IOP1, and (d) GoAmazon 2014 to 2015. CAPE is represented by red dots, while dCAPE is represented by blue dots. The air parcel launch level is determined by ULL. Correlation coefficients (corr) between CAPE and precipitation (red) and dCAPE and precipitation (blue) are also marked on the plots.

precipitation in summer at SGP. Corresponding to the strong precipitation hours, both regimes show strong advective cooling at middle and upper troposphere and strong advective moistening at lower and middle troposphere, particularly on nighttime precipitation days. It is interesting to see that the maximum advective cooling is generally in phase with precipitation peak, while the maximum advective moistening appears a few hours earlier than precipitation peak, in particular, for afternoon precipitation, acting to precondition the environment for these convective events. In contrast, the large-scale forcing is weaker over dry periods than wet periods on both afternoon and nighttime precipitation days. In general, there is moderate advective warming/drying at middle and low levels, which is not in favor of convection.

The diurnal composites of CAPE and dCAPE calculated with an air parcel that is launched at different vertical levels from surface to 600 hPa for the two precipitation regimes at SGP are shown in Figure 6. Large CAPE is seen between 1200 and 2100 LST near the surface on afternoon deep convection days (Figure 6a), consistent with the fact that afternoon deep convection is primarily driven locally by surface fluxes (Y. Zhang & Klein, 2010). Similar structure is seen on nighttime precipitation days (Figure 6b), but the maximum CAPE appears later around the hours between 1500 LST and midnight, suggesting that convection could be wrongly triggered in late afternoon with CAPE-based trigger. Consistent with the fact that nocturnal convection at SGP is often elevated and occurs around midnight, the vertical extent of having strong CAPE at midnight is also higher on nighttime precipitation days than on afternoon precipitation days.

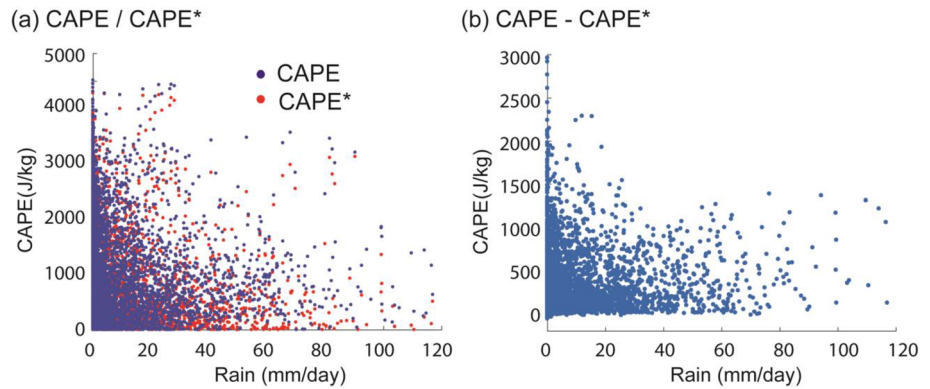


**Figure 3.** (a) The scatter plots of CAPE versus precipitation for JJA 2004–2015 at the SGP site. CAPE calculated with the surface-based assumption (CAPE\*) is marked as red, while CAPE with the ULL-based assumption (CAPE) is marked as blue. (b) The scatter plot of the CAPE difference between the surface-based and ULL-based assumptions (i.e., CAPE - CAPE\*) with respect to precipitation.

Positive dCAPE again corresponds to precipitation much better than CAPE for both precipitation regimes, where negative dCAPE is typically shown over dry periods, acting to suppress deep convection. Positive dCAPE is much stronger and extends much deeper on nighttime precipitation days than afternoon precipitation days. This is consistent with the much stronger large-scale forcing associated with the nocturnal peak on nighttime deep convection days as discussed earlier. The strong positive dCAPE indicates a strong destabilization of the atmosphere due to the passage of MCSs at night.

Precipitation starts and peaks a few hours earlier (later) at MAO than at SGP on afternoon deep convection days (nighttime deep convection days) (Figure 7). It is interesting to see a secondary precipitation peak around 1400 LST shown on nighttime convection days, likely related to remaining precipitation from previous nocturnal events or afternoon convection happening on the day of nocturnal convection.

The associated large-scale forcing fields exhibit quite distinct features between afternoon and nighttime deep convection regimes and also are quite different from what are seen at SGP. On afternoon precipitation days, strong advective cooling is seen at middle and upper troposphere, while strong advective moistening is only seen at the level above 700 hPa. Below 700 hPa, there is moderate advective drying. It is seen that strong low-level moistening occurs prior to deep convection. On nighttime precipitation days, corresponding to nocturnal precipitation, advective cooling and moistening during the strong precipitation hours are mainly located at lower and middle troposphere, lower than those seen on afternoon precipitation days. During the day, moderate advective warming and drying are found in the lower troposphere.

The feature of the diurnal composite of CAPE/dCAPE at MAO (Figure 8) is similar to that shown at SGP. Positive dCAPE is a much better measure than CAPE for convection onset on both afternoon and nighttime deep convection days. Over dry periods, strong negative dCAPE is detected, acting to suppress deep convection. Furthermore, dCAPE extends much deeper on nighttime precipitation days than afternoon precipitation days, suggesting the existence of elevated convection for nighttime precipitation over tropical land.

In summary, the ARM observations show strong observational evidence to the convective triggering mechanisms implied in the dCAPE&ULL trigger that was introduced in Xie et al. (2019). In the next section, we test its performance in modeling precipitation and its diurnal variations over different deep convection regimes under the SCM framework.

Event of 2011-04-24

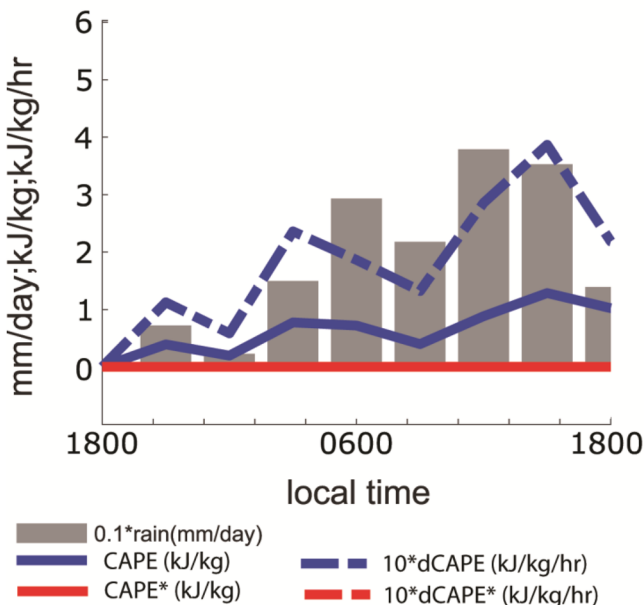


**Figure 4.** Time series of CAPE and dCAPE of the elevated convection event on 24–25 April 2011 during MC3E. CAPE and dCAPE calculated from surface (i.e., CAPE\* and dCAPE\*) are marked as red, while those calculated with the launch level determined by ULL (i.e., CAPE and dCAPE) are marked as blue. Observed precipitation is plotted as gray bars.

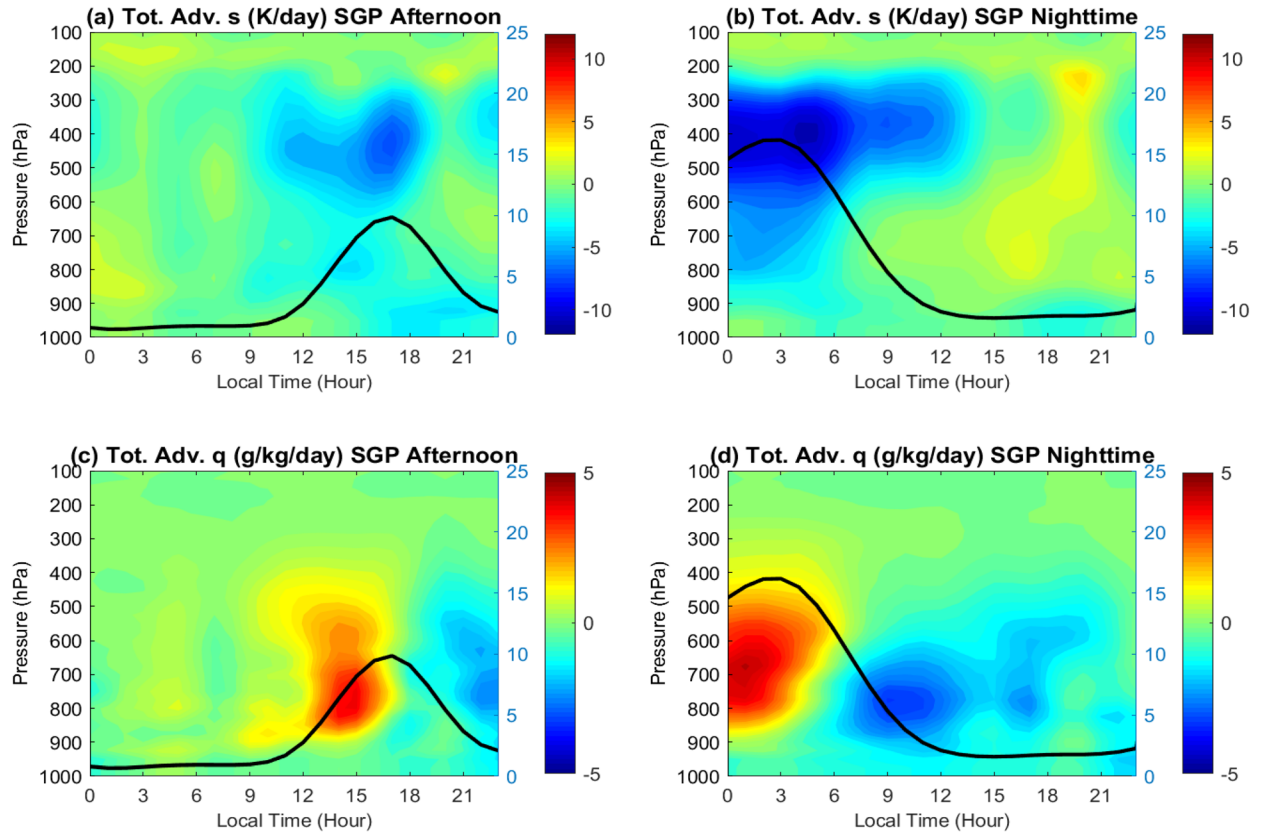


**Figure 5.** Diurnal cycle of (a, b) total advections of dry static energy  $s$  and (c, d) total advections of moisture  $q$  composite for afternoon and nighttime precipitation regimes during 2004–2015 JJA at SGP. Black line and the right y axis show the composite precipitation rate (mm/day).

## 5. SCM Test

SCM is a useful tool in testing physical parameterizations as the advective forcing can be specified from the observations (Randall et al., 1996). It can help evaluate responses of model physics to observed forcing without possible model dynamical error introduced by the feedback between convection and dynamical fields. The SCM approach has been widely used in the modeling community to identify model deficiencies in simulating various convective systems in different climate regimes through multimodel intercomparison studies (Davies et al., 2013; Fridlind et al., 2012; Ghan et al., 2000; Xie et al., 2002; Xie et al., 2005; Xu et al., 2005). By specifying the advective tendencies from observations, the local tendencies of temperature  $T$  and moisture  $q$  within the column are determined by physical tendencies from model physical parameterizations in an SCM:

$$\frac{\partial T}{\partial t} = \left( \frac{\partial T}{\partial t} \right)_{HLS} - \omega \left( \frac{\partial T}{\partial p} - \frac{RT}{pc_p} \right) + \left( \frac{\partial T}{\partial t} \right)_{phy} \quad (3)$$

and

$$\frac{\partial q}{\partial t} = \left( \frac{\partial q}{\partial t} \right)_{HLS} - \omega \left( \frac{\partial q}{\partial p} \right) + \left( \frac{\partial q}{\partial t} \right)_{phy} \quad (4)$$

where  $\omega$  is pressure vertical velocity, which can be specified from the observations or calculated by the model. The terms with *HLS* represent the observed large-scale horizontal advective forcing, and those with *physics* represent the tendency produced by physical parametrization.

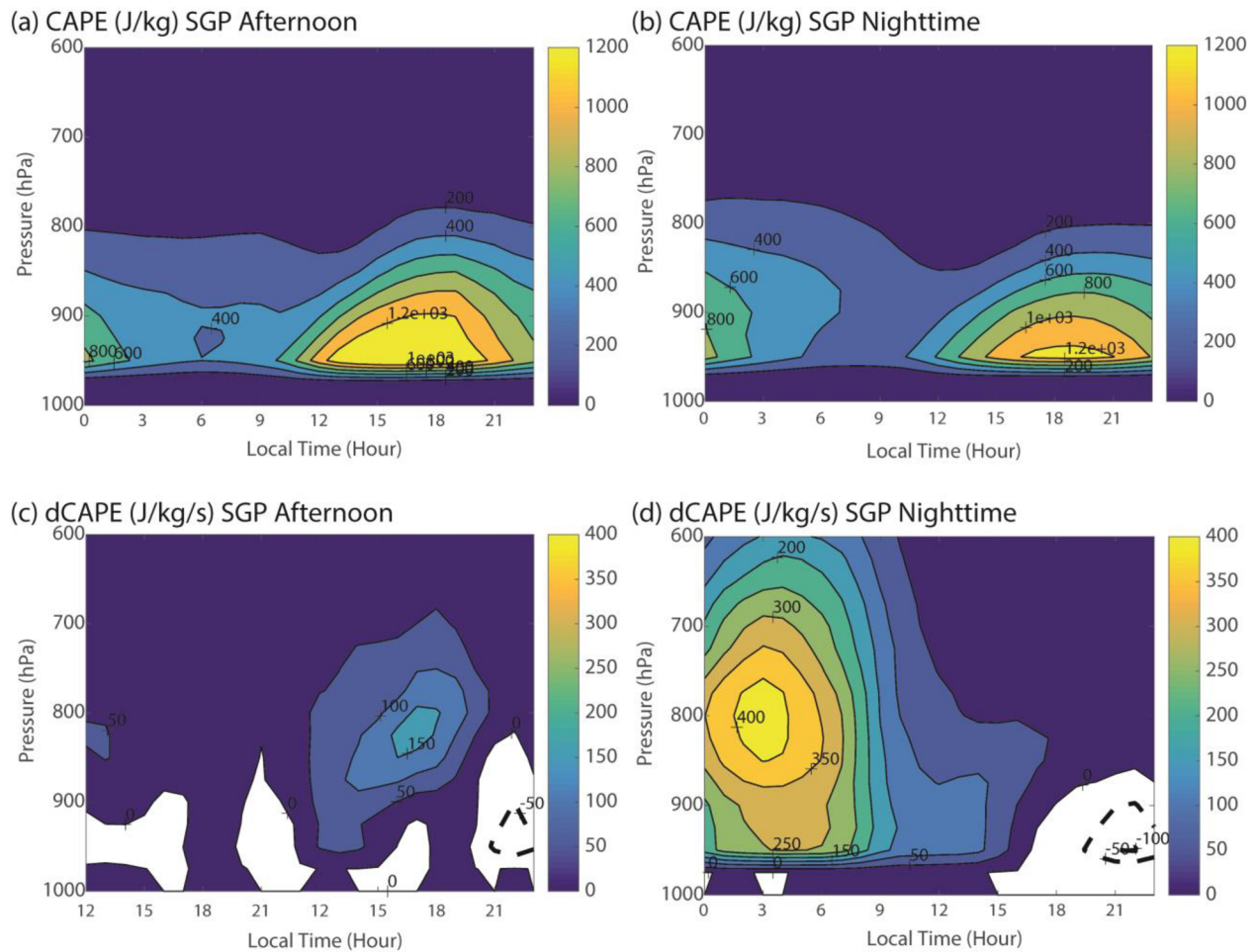


**Figure 6.** Composite of diurnal variation of CAPE and dCAPE for afternoon and nighttime precipitation regimes at the SGP site identified from the ARM observational data set from JJA 2004 to 2015. Panels (a) and (b) show CAPE for afternoon regime and nighttime regime, respectively, while panels (c) and (d) show dCAPE for the two regimes. In the figures, negative dCAPE is represented by dashed lines.

### 5.1. The E3SM SCM and Experiment Design

The model used in this study is the SCM version of E3SM version 1 (E3SM-SCM), which was recently developed by the Department of Energy. Its atmospheric component (EAMv1) is built upon CAM5.3 with improved physical parameterizations and increased model resolution (Rasch et al., 2019; Xie et al., 2018). Specifically, a third-order turbulence closure parameterization named Cloud Layers Unified By Binormals (Golaz et al., 2002; Larson & Golaz, 2005) is used in EAMv1 as a unified scheme for planetary boundary layer turbulence, shallow convection, and cloud macrophysics along with the updated Morrison and Gettelman cloud microphysics scheme (Gettelman & Morrison, 2015) for stratiform clouds. The deep convection scheme is the ZM scheme whose implementation in EAMv1 is still the same as that used in CAM5 (Neale et al., 2008). Given the changes in both model physics and model resolution, several adjustable parameters used in CAM5 were retuned in EAMv1 to make the global radiative energy budget balance and produce a reasonable climate. Xie et al. (2018), Qian et al. (2018) and Zhang et al. (2019) provided more detailed information about its tuning strategy and simulated convective processes and clouds.

EAMv1 was found to have difficulties in capturing the observed diurnal cycle of precipitation and propagation of mesoscale convective systems in both midlatitude and tropics, particularly the nocturnal peaks over these regions (Rasch et al., 2019; Tang, Klein, et al., 2019; Zheng et al., 2019). With the revised convective trigger for ZM, Xie et al. (2019) showed that the phase of diurnal cycle of precipitation simulated by EAMv1 was significantly improved. However, the amplitude of diurnal cycle of precipitation is still too

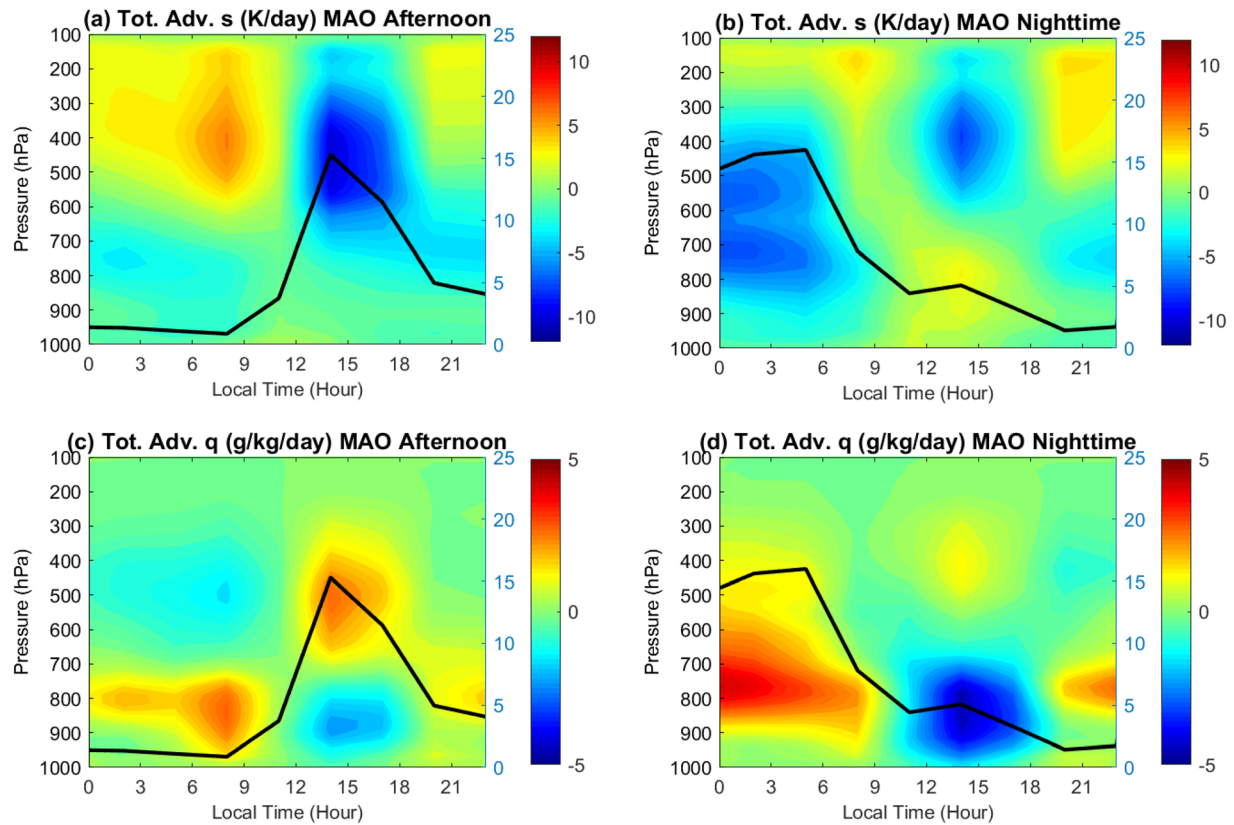


Figure 7. Same as Figure 5 but for ARM MAO site.

weak compared to observations, which might be related to the biased large-scale structures in long-term climate simulations.

In this study, we perform a series of 36-hr simulations with the SCM initialized every day at 00Z, similar to the short-range hindcast approach used in Xie, Cederwall, and Zhang (2004) and the ensemble framework used in Hume and Jakob (2005) and Y. C. Wang et al. (2015), to keep the large-scale state close to the observations so that model errors could mostly be attributed to deficiencies in model physical parameterizations. With a spin-up time of 12 hr, the analysis data are composed of an ensemble of 12- to 36-hr simulations. The dCAPE&ULL trigger is tested for both IOPs and multiyear periods at the two ARM sites with the forcing data described in Table 1 for both the case study and the statistical analysis. Details of the SCM runs are summarized in Table 2.

## 5.2. Case Study

Figure 9 shows the E3SM-SCM simulated total precipitation (PRECT) and its convective component (PRECC) with the dCAPE&ULL trigger and the default trigger for MC3E. They both well capture the total precipitation over the MC3E period. Note that this is a common feature in a single-column modeling framework, where the total precipitation is mostly controlled by the specified large-scale forcing. However, the precipitation partition differs significantly in these two runs. More convective precipitation is produced with the dCAPE&ULL trigger, particularly for the nocturnal elevated cases (e.g., the case marked by the black arrow).

To further illustrate this, Figure 10 shows the model simulated precipitation and CAPE/dCAPE for the 24–25 April nocturnal elevated convective case. It is seen that the default model fails to produce any convective precipitation, while the new trigger starts to show the capability to capture the elevated convection at night. As discussed earlier, the elevated convective event occurred in a rather stable environment where the boundary layer was very dry, and the convection was decoupled from the surface. By removing the restriction for

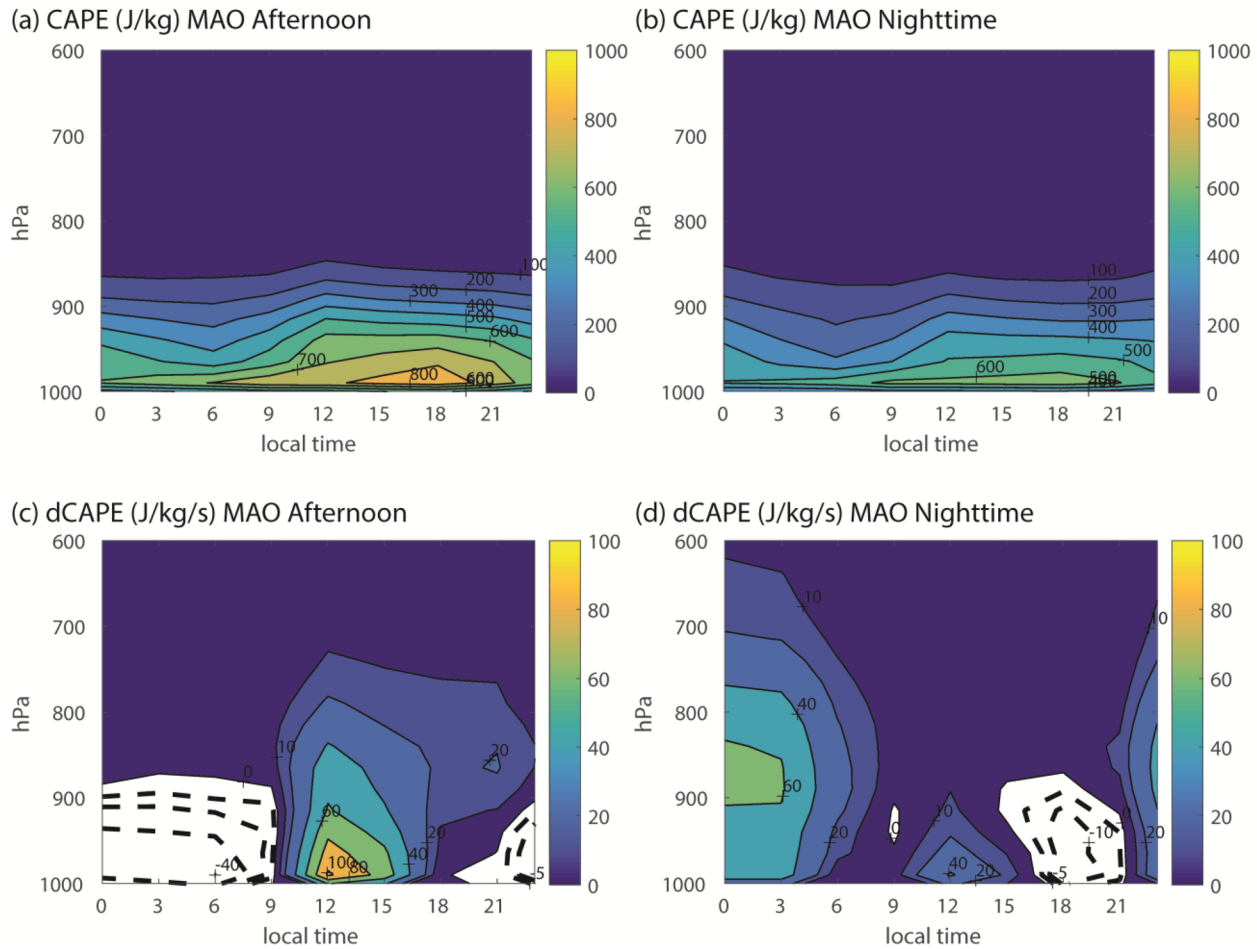
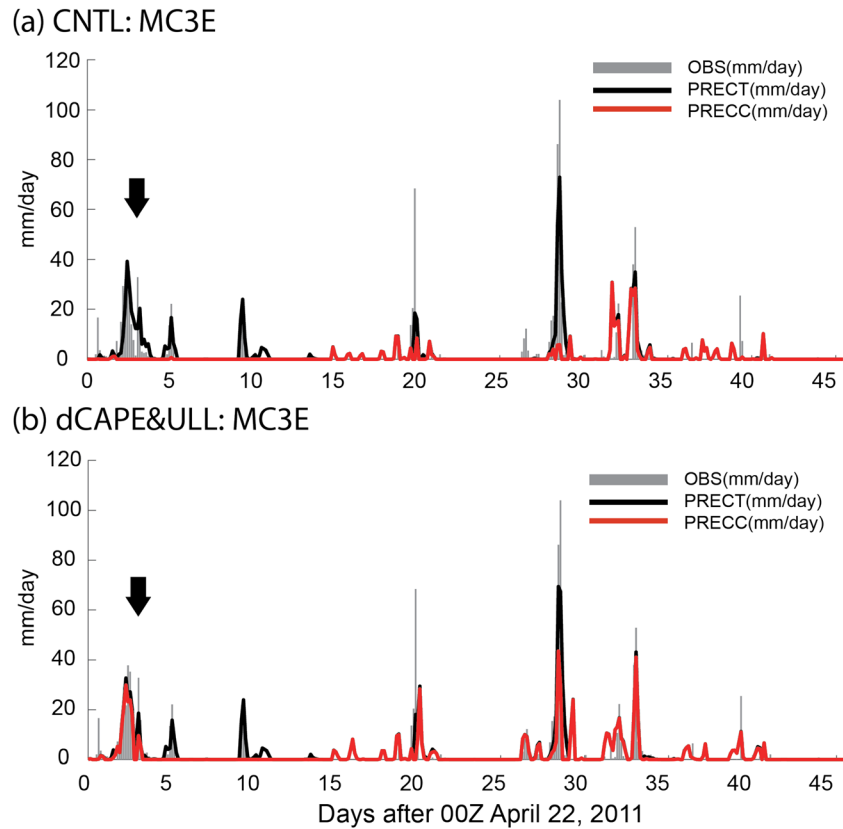


**Figure 8.** Composite of diurnal variation of CAPE and dCAPE for afternoon and nighttime regimes at the MAO site identified from the 2-year GoAmazon period from 2014 to 2015. Panels (a) and (b) show CAPE for afternoon regime and nighttime regime, respectively, while panels (c) and (d) show dCAPE for the two regimes. In the figures, negative dCAPE is represented by dashed lines.

convection to have its root in the boundary layer, as assumed in the default ZM scheme, the model with the dCAPE&ULL trigger is able to efficiently capture the elevated convective event, consistent with what is shown in Figure 4 based on the observations.

**Table 2**  
Summary of SCM Runs

Model ID	Description	Convective trigger
CNTL	Default EAMv1 (Rasch et al., 2019, Xie et al., 2018)	(1) CAPE > 70 J/kg (2) The air parcel launch level is chosen within the boundary layer
dCAPE&ULL	CNTL with the dCAPE&ULL trigger (Xie et al., 2019)	(1) CAPE > 0 (2) dCAPE > 0 (3) The air parcel launching level is chosen between the surface and 600 hPa
dCAPE	CNTL with the dCAPE trigger only (Xie & Zhang, 2000)	(1) CAPE > 0 (2) dCAPE > 0 (3) The air parcel launch level is chosen within the boundary layer
ULL	CNTL with the ULL trigger only (Y. C. Wang et al., 2015)	(1) CAPE > 70 J/kg (2) The air parcel launching level is chosen between the surface and 600 hPa



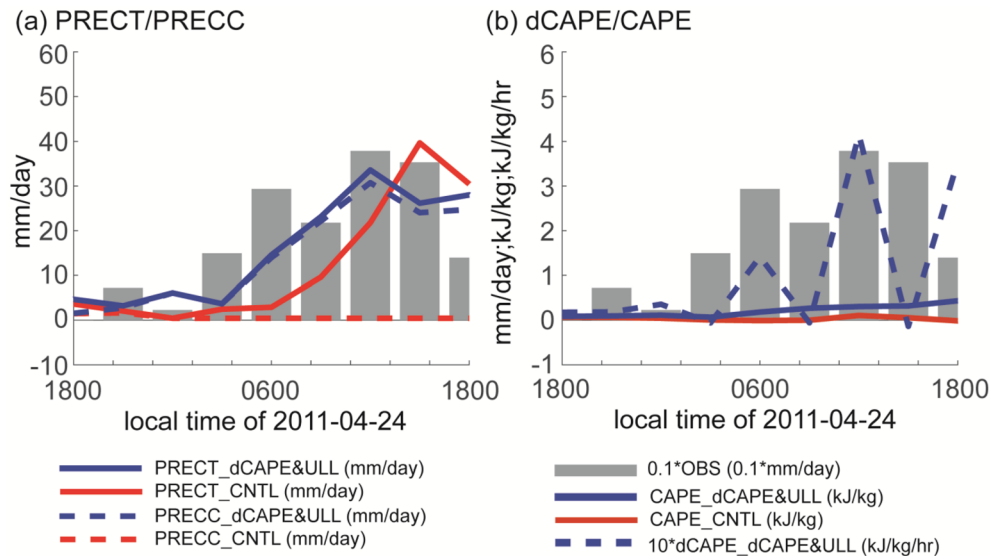
**Figure 9.** Time series of total precipitation (PRECT; black line) and convective precipitation (PRECC; red line) simulated by the (a) CNTL and the (b) dCAPE&ULL triggers in the ZM scheme for the MC3E field campaign. Gray bar shows the observations from the ARM site. The black arrow indicates the elevated convection event on 24–25 April 2011 shown in Figure 4.

Figure 11 shows time series of precipitation between the 13th and 23rd days during the GoAmazon IOP1 which contains two strong nocturnal convective events that occurred on day 15 (i.e., 1 March 2014) and day 21 (i.e., 7 March 2014). Similar to the MC3E case, both the default and revised models well capture the observed total precipitation rates, while they differ significantly in convective precipitation for the two strong nocturnal precipitation events. Over these two periods, the total precipitation simulated by the default model is almost purely from the resolved-scale precipitation, while it is mainly from the convective precipitation in the revised model. Although the difference in the total precipitation produced by these two triggers is small in the single-column setup for the reason we mentioned earlier, the difference in their precipitation partitioning would result in a very different dynamical response in global simulations (e.g., Lin et al., 2013; Wu et al., 2000).

### 5.3. Diurnal Cycle of Precipitation

The diurnal cycles of precipitation simulated by the E3SM-SCM with various convective triggers (CNTL, dCAPE&ULL, dCAPE, and ULL) over the SGP and MAO sites are shown in Figure 12. To make sure that the diurnal cycle of precipitation is of representative of these two regions, the models are run for multiple years so that we have sufficient samplings to generate the diurnal composites. Specifically, the models are run for 12 summer seasons (JJA) from 2004 to 2015 at SGP and the entire 2 years (2014–2015) at MAO with the ARM continuous forcing data described in Table 1.

At SGP, the ARM observation exhibits a nocturnal precipitation peak at 0300 LST in summer, while the default scheme produces a morning peak around 1000 LST and fails to capture the observed nocturnal peak (Figure 12a). It is seen that almost no convection is triggered at night as indicated by the convective



**Figure 10.** Time series of simulated precipitation and CAPE/dCAPE of the elevated convection events on 24–25 April 2011 during MC3E in the single-column model runs. (a) Convective (dotted) and total precipitation (solid) calculated with the revised trigger (dCAPE&ULL; blue lines) and the default trigger (CNTL; red lines). (b) dCAPE (dotted) and CAPE (solid) with the revised trigger (dCAPE&ULL; blue lines) and CAPE with the default trigger (CNTL; red solid line). The observed precipitation is plotted as gray bars.

precipitation component (Figure 12c). This problem is largely reduced with dCAPE&ULL, which well reproduces the nocturnal peak at 0300 LST due to the capture of elevated convection. The respective roles of dCAPE and ULL on the diurnal cycle over the SGP are also shown in the figure. As expected, dCAPE trigger acts to suppress daytime precipitation, primarily contributing to the reduction of convective precipitation, while the ULL trigger is essential for capturing nocturnal convective precipitation. Interestingly, the ULL trigger also plays a dominant role in reducing daytime precipitation, attributing to the release of unstable energy at night. With the specified large-scale forcing, the amplitude of the diurnal cycle is also well captured by the dCAPE&ULL trigger.

Over the tropical site, convection develops much faster in the default model than the observation during the day (Figure 12b). The model precipitation peaks in the early morning (0900 LST) compared to the observed afternoon peak (1400 LST). There is no convection triggered between 2100 and 0700 LST at night (Figure 12d). In contrast, the dCAPE&ULL trigger shows a much better skill in capturing the observed daytime peak and nighttime precipitation. The improved feature with dCAPE&ULL is primarily from the use of ULL, which helps both capture nocturnal precipitation and suppress daytime precipitation, similar to what have been seen at SGP. The dCAPE trigger slightly reduces the overestimated precipitation in early morning and increases the precipitation amount in the afternoon, resulting in a slightly improved diurnal cycle compared to the default scheme.

The model behaviors with different convective triggers can be even more clearly demonstrated for the two precipitation regimes that we discussed in section 4 (Figure 13). In both regimes, the dCAPE&ULL trigger effectively suppresses the spurious precipitation during the day and captures well the timing and amplitude of the observed precipitation peak in later afternoon (midnight) on afternoon precipitation days (nighttime precipitation days). Both dCAPE and ULL contribute to the improvements, while ULL plays the dominant roles for both SGP and MAO sites. It is noted that the model may overestimate nocturnal precipitation on afternoon deep convection days with ULL, which is an issue that has not been discussed in Xie et al. (2019).

#### 5.4. Precipitation Intensity Distribution

Figure 14 shows the precipitation intensity distributions during daytime (i.e., 0080–1800 LST) and nighttime (i.e., 2000–0600 LST) over the 12 summers at SGP and the 2-year period at MAO. At SGP, the default model

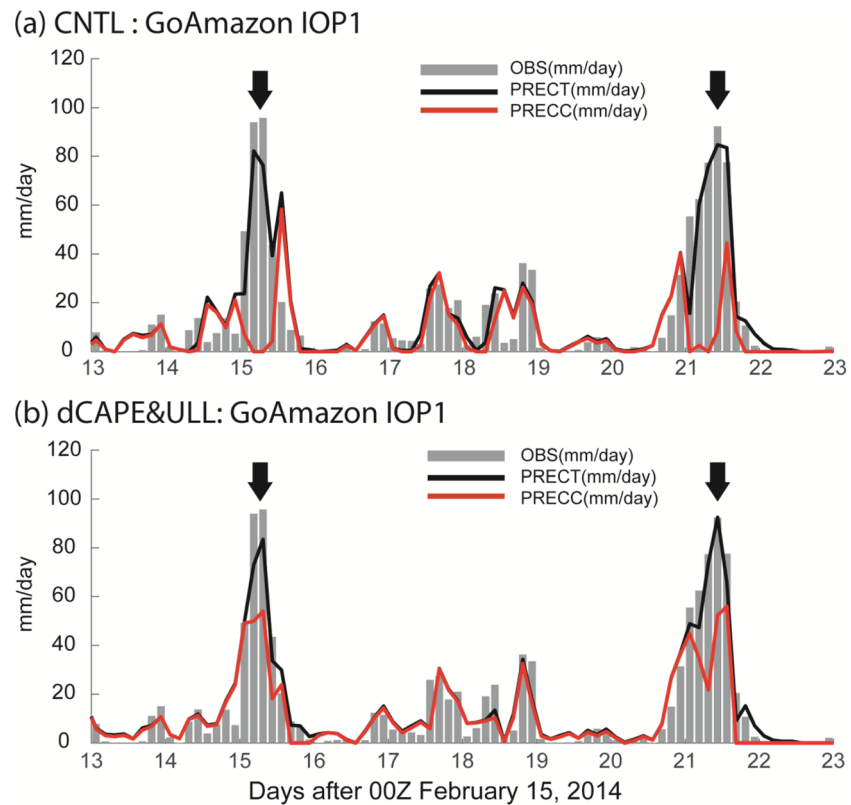


**Figure 11.** Same as Figure 9 except for the GoAmazon IOP1. The black arrows mark the events on 1 March and 7 March event mentioned in the text.

largely overestimates the frequency of the observed daytime precipitation for almost all the categories except for precipitation rates  $< 2$  mm/day (Figure 14a), while it underestimates the frequency of the observed nighttime precipitation that is larger than 10 mm/day (Figure 14b). The overestimation of daytime precipitation, in particular for precipitation rates  $> 10$  mm/day, has been largely reduced by the dCAPE&ULL trigger, primarily due to the use of ULL. The dCAPE plays a very minor role in suppressing the spurious daytime precipitation in this range at the midlatitude site. For nighttime precipitation, the dCAPE&ULL trigger increases the occurrence of precipitation events for all categories and well captures the observed moderate-to-heavy nocturnal precipitation ( $> 10$  mm/day) compared to the default run, again due to the use of ULL.

Similar to SGP, the default model largely overestimates daytime precipitation between 2 and 20 mm/day at the tropical site (MAO), while it underestimates intense nighttime precipitation with precipitation rates  $> 20$  mm/day (Figures 14c and 14d). The dCAPE&ULL trigger almost perfectly reproduces the observed precipitation intensity distribution for daytime precipitation due to the contribution from both dCAPE and ULL while it only captures well the heavy precipitation ( $> 20$  mm/day) at night. Compared to SGP, the dCAPE trigger acts more effectively to suppress the spurious precipitation produced by the default trigger at MAO. It is interesting to see that the use of ULL has led to a large overestimation of light-to-moderate precipitation (1–10 mm/day) for all the cases. This problem can also be seen in Figures 12b and 13b for nocturnal precipitation. Overall, the combined scheme (dCAPE&ULL) produces the best results for all the features that we examined.

## 6. Summary and Discussion

In this study, we conducted a comprehensive observational analysis and SCM tests to better understand the characteristics of the revised convective trigger, dCAPE&ULL, described in Xie et al. (2019). The

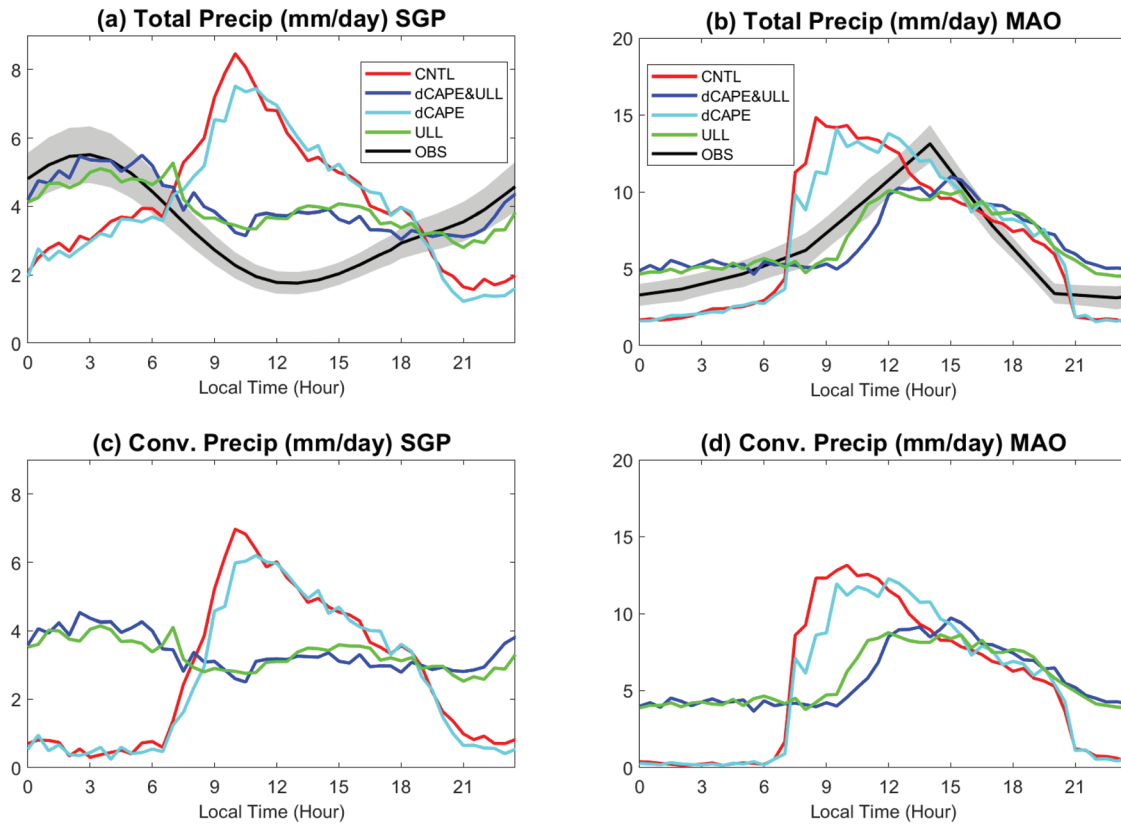


**Figure 12.** Comparison of mean diurnal precipitation cycle of (a) total precipitation for JJA 2004–2015 at SGP, (b) total precipitation for GoAmazon 2014–2015 at MAO, (c) convective precipitation for JJA 2004–2015 at SGP, and (d) convective precipitation for GoAmazon 2014–2015 at MAO, simulated from E3SM-SCM with various convective triggers. Observed total diurnal precipitation cycle is shown in black with shading indicates standard error.

dCAPE&ULL trigger consists of a dynamic CAPE trigger (dCAPE) with an ULL to prevent convection from being triggered too frequently during the day (dCAPE) and allow elevated convection to be captured at night (ULL). Both ARM MC3E and GoAmazon field campaign data and long-term observations at its SGP and MAO sites were used for evaluating the revised trigger. The E3SM-SCM was used to test its performance in modeling precipitation and its diurnal variations over different deep convection regimes.

The ARM observations show strong evidence of a close correlation between convection initiation and the positive dCAPE, indicating a strong coupling between convection and the large-scale dynamic forcing that is implied by the dCAPE trigger. Using the dCAPE trigger can largely alleviate the unrealistically strong coupling of convection to surface heating, which is thought to be one of the major reasons for the failure of capturing diurnal cycle of precipitation in current climate models. The observations also show that removing the restriction of convection being rooted within the boundary by ULL is essential for capturing elevated convection which commonly occurs at night due to the passage of MCSs. The regime analysis on afternoon deep convection days and nighttime deep convection days further demonstrates that combining the dCAPE trigger with ULL would allow precipitation to be better simulated in climate models.

Consistent with what are illustrated in the observations, SCM tests show that the dCAPE trigger acts to suppress daytime convection, in particular for tropical convective systems, while the ULL trigger is the key to capturing nocturnal elevated convection. Likely due to the release of unstable energy at night, the spurious morning precipitation shown in the default model is also significantly reduced with the use of ULL on afternoon precipitation days. The combination of these two processes in the dCAPE&ULL trigger gives an overall

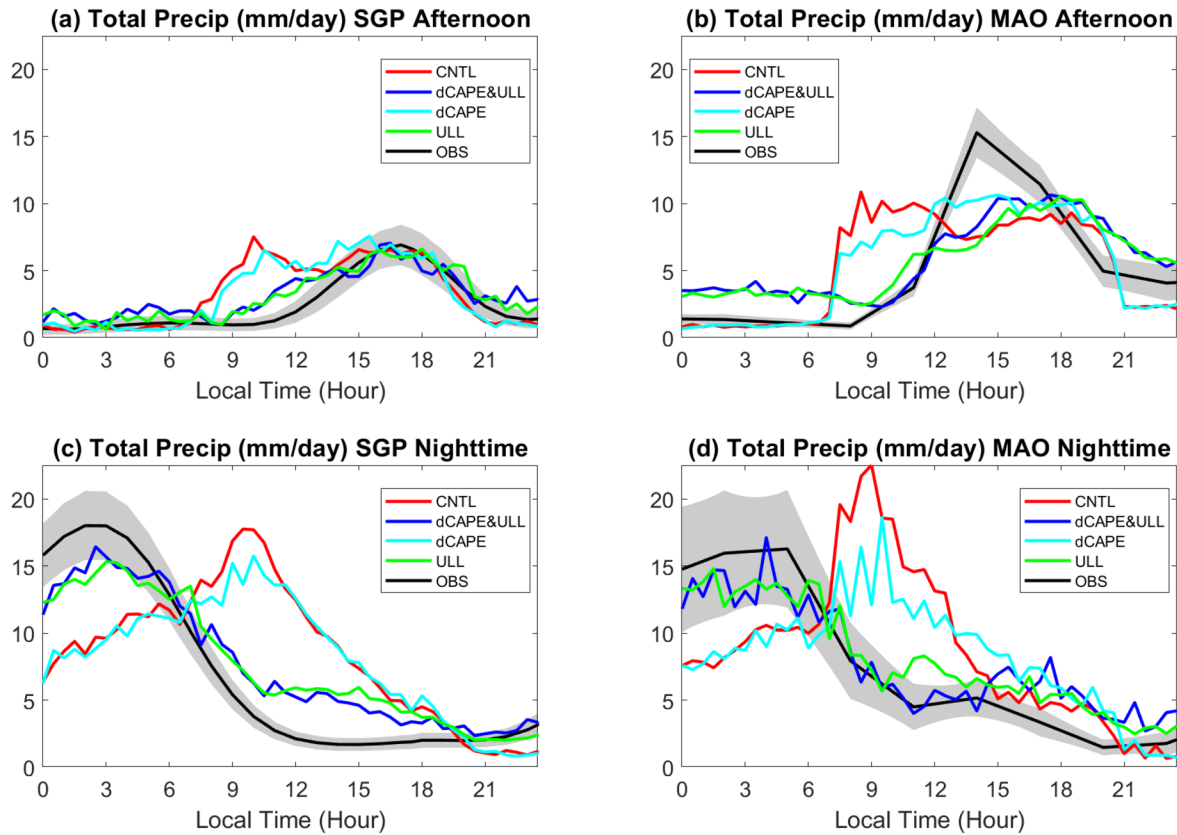


**Figure 13.** Mean diurnal total precipitation for (a) afternoon precipitation composite for JJA 2004–2015 at SGP, (b) afternoon precipitation composite for GoAmazon 2014–2015 at MAO, (c) nighttime precipitation composite for JJA 2004–2015 at SGP, and (d) nighttime precipitation composite for GoAmazon 2014–2015 at MAO, simulated from E3SM-SCM with various convective triggers. Observed total diurnal precipitation cycle is shown in black with shading indicates standard error.

better performance than the individual changes, similar to what have been shown in Xie et al. (2019). This suggests that the suppression of convection during the day by dCAPE acts to preserve instability for nighttime intense convection, and in turn, the release of convective instability at night results in less CAPE available for daytime convection. It is also noteworthy that impacts of the proposed convective trigger on precipitation may be underestimated in an SCM framework because model precipitation is largely controlled by the enforced large-scale forcing. Nevertheless, the major features shown in Xie et al. (2019) are largely reproduced under the SCM framework. One issue that has not been explored in Xie et al. (2019) is that the use of ULL could lead to an overestimation of light-to-moderate precipitation (1–10 mm/day) due to more convection being triggered above boundary layer than the default scheme, which needs to be investigated further in the full E3SM.

It should be noted that dCAPE-based triggers may not work well for convection that has weak connection with its large-scale environment. A recent study by Song et al. (2019) found that the connection between convection and large-scale forcing has weakened substantially over the Great Plains during summertime, indicated by the weak correlation between MCS and surface CAPE anomalies. This may imply that dCAPE-based triggers might have difficulties in capturing MCSs over that region. However, the situation often happens for nocturnal elevated convection, which is typically associated with the propagation of MCS and/or enhanced Great Plain Low-Level Jet, where CAPE is hardly detected for an air parcel lifting from the surface as shown in the current study. Combining ULL with the dCAPE trigger as suggested in Xie et al. (2019) can largely address this issue and allow the elevated convection to be realized. Another issue with the dCAPE&ULL trigger is that its performance could be resolution dependent since dCAPE can often be dominated by grid-scale vertical velocity which is sensitive to model horizontal resolution (Song &

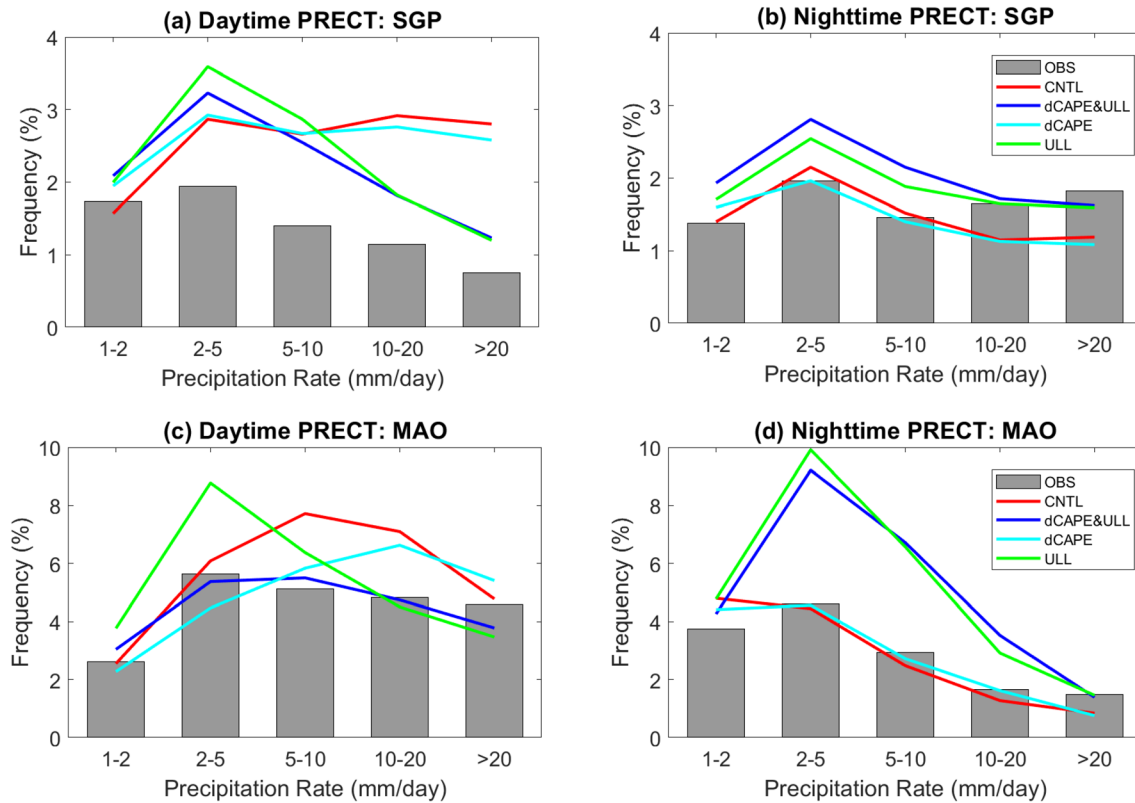


**Figure 14.** (a, c) Daytime and (b, d) nighttime occurrence frequency for different total precipitation rates for (a, b) 2004–2015 JJA at SGP and (c, d) GoAmazon 2014–2015 at MAO. Daytime is defined as 8 a.m. to 6 p.m., and nighttime is defined as 8 p.m. to 6 a.m. 3-hour data samples are used.

#### Acknowledgments

This research was primarily supported as part of the Energy Exascale Earth System Model (E3SM) project and partially supported by the Climate Model Development and Validation activity and Atmospheric Radiation Measurement (ARM) program, funded by the U.S. Department of Energy, Office of Science, Office of Biological and Environmental Research. All model data presented in this study can be obtained online (<https://portal.nersc.gov/project/m2136/E3SMv1/Wang-newTrigger/>). We thank Peter Bogenschutz for providing the updated E3SM SCM code. We benefit from the discussion with Chris Golaz, Xue Zheng, and Hsi-Yen Ma during the course of study. We also thank the two anonymous reviewers for constructive comments. Work at LLNL was performed under the auspices of the U.S. DOE by Lawrence Livermore National Laboratory under contract DE-AC52-07NA27344. Dr. Yi-Chi Wang is also supported by the Ministry of Science and Technology, Taiwan, under Grants MOST 105-2119-M-001-018 and 107-2111-M-001-010.

Zhang, 2017; 2018). How to make the dCAPE&ULL trigger scale aware is another subject that warrants future study, which may include the introduction of a resolution-dependent threshold for dCAPE and the consideration of the history of convection as suggested in Song and Zhang (2018).

#### References

- Bechtold, P., Semane, N., Lopez, P., Chaboureaud, J.-P., Beljaars, A., & Bormann, N. (2014). Representing equilibrium and nonequilibrium convection in large-scale models. *Journal of the Atmospheric Sciences*, *71*(2), 734–753. <https://doi.org/10.1175/JAS-D-13-0163.1>
- Davies, L., Jakob, C., Cheung, K., Genio, A. D., Hill, A., Hume, T., et al. (2013). A single-column model ensemble approach applied to the TWP-ICE experiment. *Journal of Geophysical Research: Atmospheres*, *118*, 6544–6563. <https://doi.org/10.1002/jgrd.50450>
- Fridlind, A. M., Ackerman, A. S., Chaboureaud, J. P., Fan, J., Grabowski, W. W., Hill, A. A., et al. (2012). A comparison of TWP-ICE observational data with cloud-resolving model results. *Journal of Geophysical Research*, *117*, D05204. <https://doi.org/10.1029/2011JD016595>
- Fritsch, J. M., & Chappell, C. F. (1980). Numerical prediction of convectively driven mesoscale pressure systems. Part I: Convective parameterization. *Journal of the Atmospheric Sciences*, *37*(8), 1722–1733. [https://doi.org/10.1175/1520-0469\(1980\)037<1722:NPOCDM>2.0.CO;2](https://doi.org/10.1175/1520-0469(1980)037<1722:NPOCDM>2.0.CO;2)
- Geerts, B., Parsons, D., Ziegler, C. L., Weckwerth, T. M., Biggerstaff, M. I., Clark, R. D., et al. (2017). The 2015 plains elevated convection at night field project. *Bulletin of the American Meteorological Society*, *98*(4), 767–786. <https://doi.org/10.1175/BAMS-D-15-00257.1>
- Gettelman, A., & Morrison, H. (2015). Advanced two-moment bulk microphysics for global models. Part I: Off-line tests and comparison with other schemes. *Journal of Climate*, *28*(3), 1268–1287. <https://doi.org/10.1175/JCLI-D-14-00102.1>
- Ghan, S., Randall, D., Xu, K. M., Cederwall, R., Cripe, D., Hack, J., et al. (2000). A comparison of single column model simulations of summertime midlatitude continental convection. *Journal of Geophysical Research*, *105*(D2), 2091–2124. <https://doi.org/10.1029/1999JD900971>
- Golaz, J.-C., Caldwell, P. M., van Roekel, L. P., Petersen, M. R., Tang, Q., Wolfe, J. D., et al. (2019). The DOE E3SM coupled model version 1: Overview and evaluation at standard resolution. *Journal of Advances in Modeling Earth Systems*, *11*, 2089–2129. <https://doi.org/10.1029/2018MS001603>
- Golaz, J. C., Larson, V. E., & Cotton, W. R. (2002). A PDF-based model for boundary layer clouds. Part I: Method and model description. *Journal of the Atmospheric Sciences*, *59*(24), 3540–3551. [https://doi.org/10.1175/1520-0469\(2002\)059<3540:APBMFB>2.0.CO;2](https://doi.org/10.1175/1520-0469(2002)059<3540:APBMFB>2.0.CO;2)
- Han, J., & Pan, H.-L. (2011). Revision of convection and vertical diffusion schemes in the NCEP global forecast system. *Weather and Forecasting*, *26*(4), 520–533. <https://doi.org/10.1175/WAF-D-10-05038.1>
- Hume, T., & Jakob, C. (2005). Ensemble single column modeling (ESCM) in the tropical western Pacific: Forcing data sets and uncertainty analysis. *Journal of Geophysical Research*, *110*, D13109. <https://doi.org/10.1029/2004JD005704>

- Jensen, M. P., Toto, T., Troyan, D., Ciesielski, P. E., Holdridge, D., Kyrrouac, J., et al. (2015). The midlatitude continental convective clouds experiment (MC3E) sounding network: Operations, processing and analysis. *Atmospheric Measurement Techniques*, *8*(1), 421–434. <https://doi.org/10.5194/amt-8-421-2015>
- Kain, J. S. (2004). The Kain-Fritsch convective parameterization: An update. *Journal of Applied Meteorology*, *43*(1), 170–181. [https://doi.org/10.1175/1520-0450\(2004\)043<0170:TKCPAU>2.0.CO;2](https://doi.org/10.1175/1520-0450(2004)043<0170:TKCPAU>2.0.CO;2)
- Kain, J. S., & Fritsch, J. M. (1992). The role of the convective “trigger function” in numerical forecasts of mesoscale convective systems. *Meteorology and Atmospheric Physics*, *49*(1–4), 93–106. <https://doi.org/10.1007/BF01025402>
- Larson, V. E., & Golaz, J. (2005). Using probability density functions to derive consistent closure relationships among higher-order moments. *Monthly Weather Review*, *133*, 1023–1042. Retrieved from: <http://journals.ametsoc.org/doi/pdf/10.1175/MWR2902.1>
- Lee, M.-I., Schubert, S. D., Suarez, M. J., Held, I. M., Lau, N. C., Ploshay, J. J., et al. (2007). An analysis of the warm-season diurnal cycle over the continental United States and Northern Mexico in general circulation models. *Journal of Hydrometeorology*, *8*(3), 344–366. <https://doi.org/10.1175/JHM581.1>
- Lee, M.-I., Schubert, S. D., Suarez, M. J., Schemm, J.-K. E., Pan, H.-L., Han, J., & Yoo, S.-H. (2008). Role of convection triggers in the simulation of the diurnal cycle of precipitation over the United States Great Plains in a general circulation model. *Journal of Geophysical Research*, *113*, D02111. <https://doi.org/10.1029/2007JD008984>
- Lin, Y., Zhao, M., Ming, Y., Golaz, J. C., Donner, L. J., Klein, S. A., et al. (2013). Precipitation partitioning, tropical clouds, and intraseasonal variability in GFDL AM2. *Journal of Climate*, *26*(15), 5453–5466. <https://doi.org/10.1175/JCLI-D-12-00442.1>
- Marshall, J. H., Trier, S. B., Weckwerth, T. M., & Wilson, J. W. (2011). Observations of elevated convection initiation leading to a surface-based squall line during 13 June IHOP\_2002. *Monthly Weather Review*, *139*(1), 247–271. <https://doi.org/10.1175/2010MWR3422.1>
- Martin, S. T., Artaxo, P., Machado, L. A. T., Manzi, A. O., Souza, R. A. F., Schumacher, C., et al. (2016). Introduction: Observations and modeling of the Green Ocean Amazon (GoAmazon2014/5). *Atmospheric Chemistry and Physics*, *16*(8), 4785–4797. <https://doi.org/10.5194/acp-16-4785-2016>
- Neale, R. B., Richter, J. H., & Jochum, M. (2008). The impact of convection on ENSO: From a delayed oscillator to a series of events. *Journal of Climate*, *21*(22), 5904–5924. <https://doi.org/10.1175/2008JCLI2244.1>
- Qian, Y., Wan, H., Yang, B., Golaz, J. C., Harrop, B., Hou, Z., et al. (2018). Parametric sensitivity and uncertainty quantification in the version 1 of E3SM atmosphere model based on short perturbed parameter ensemble simulations. *Journal of Geophysical Research: Atmospheres*, *123*, 13,046–13,073. <https://doi.org/10.1029/2018JD028927>
- Randall, D. A., & Wang, J. (1991). The moist available energy of a conditionally unstable atmosphere. *Journal of the Atmospheric Sciences*, *49*(3), 240–255.
- Randall, D. A., Xu, K., Somerville, R. J. C., & Iacobellis, S. (1996). Single-column models and cloud ensemble models as links between observations and climate models. *Journal of Climate*, *9*(8), 1683–1697. [https://doi.org/10.1175/1520-0442\(1996\)009<1683:SCMACE>2.0.CO;2](https://doi.org/10.1175/1520-0442(1996)009<1683:SCMACE>2.0.CO;2)
- Rasch, P. J., Xie, S., Ma, P. L., Lin, W., Wang, H., Tang, Q., et al. (2019). An overview of version 1 of DOE E3SM atmosphere model (EAMV1). *Journal of Advances in Modeling Earth Systems*, *11*, 2377–2411. <https://doi.org/10.1029/2019MS001629>
- Sakaguchi, K., Leung, L. R., Burleyson, C. D., Xiao, H., & Wan, H. (2018). Role of troposphere-convection-land coupling in the Southwestern Amazon precipitation bias of the Community Earth System Model Version 1 (CESM1). *Journal of Geophysical Research: Atmospheres*, *123*, 8374–8399. <https://doi.org/10.1029/2018JD028999>
- Song, F., Feng, Z., Leung, L. R., Houze, R. A. Jr., Wang, J., Hardin, J., & Homeyer, C. R. (2019). Contrasting spring and summer large-scale environments associated with mesoscale convective systems over the U.S. Great Plains. *Journal of Climate*, *32*(20), 6749–6767. <https://doi.org/10.1175/JCLI-D-18-0839.1>
- Song, F., & Zhang, G. J. (2017). Improving trigger functions for convective parameterization schemes using GOAmazon observations. *Journal of Climate*, *30*(21), 8711–8726. <https://doi.org/10.1175/JCLI-D-17-0042.1>
- Song, F., & Zhang, G. J. (2018). Understanding and improving the scale dependence of trigger functions for convective parameterization using cloud-resolving model data. *Journal of Climate*, *31*(18), 7385–7399. <https://doi.org/10.1175/JCLI-D-17-0660.1>
- Suhas, E., & Zhang, G. J. (2014). Evaluation of trigger functions for convective parameterization schemes using observations. *Journal of Climate*, *27*(20), 7647–7666. <https://doi.org/10.1175/JCLI-D-13-00718.1>
- Surcel, M., Berenguer, M., & Zawadzki, I. (2010). The diurnal cycle of precipitation from continental radar mosaics and numerical weather prediction models. Part I: Methodology and seasonal comparison. *Monthly Weather Review*, *138*(8), 3084–3106. <https://doi.org/10.1175/2010MWR3125.1>
- Tang, Q., Klein, S. A., Xie, S., Lin, W., Golaz, J. C., Roesler, E. L., et al. (2019). Regionally refined test bed in E3SM atmosphere model version 1 (EAMv1) and applications for high-resolution modeling. *Geoscientific Model Development*, *12*(7), 2679–2706. <https://doi.org/10.5194/gmd-12-2679-2019>
- Tang, S., Xie, S., Zhang, M., Tang, Q., Zhang, Y., Klein, S. A., et al. (2019). Differences in eddy-correlation and energy-balance surface turbulent heat flux measurements and their impacts on the large-scale forcing fields at the ARM SGP site. *Journal of Geophysical Research: Atmospheres*, *124*, 3301–3318. <https://doi.org/10.1029/2018JD029689>
- Tang, S., Xie, S., Zhang, Y., Zhang, M., Schumacher, C., Upton, H., et al. (2016). Large-scale vertical velocity, diabatic heating and drying profiles associated with seasonal and diurnal variations of convective systems observed in the GoAmazon2014/5 experiment. *Atmospheric Chemistry and Physics*, *16*(22), 14,249–14,264. <https://doi.org/10.5194/acp-16-14249-2016>
- Wang, J., & Randall, D. A. (1994). The moist available energy of a conditionally unstable atmosphere. Part II: Further analysis of GATE data. *Journal of the Atmospheric Sciences*, *51*(5), 703–710. [https://doi.org/10.1175/1520-0469\(1994\)051<0703:TMAEOA>2.0.CO;2](https://doi.org/10.1175/1520-0469(1994)051<0703:TMAEOA>2.0.CO;2)
- Wang, Y. C., Pan, H. L., & Hsu, H. H. (2015). Impacts of the triggering function of cumulus parameterization on warm-season diurnal rainfall cycles at the Atmospheric Radiation Measurement Southern Great Plains Site. *Journal of Geophysical Research: Atmospheres*, *120*, 10,681–10,702. <https://doi.org/10.1002/2015JD023337>
- Wu, Z., Sarachik, E. S., & Battisti, D. S. (2000). Vertical structure of convective heating and the three-dimensional structure of the forced circulation on an equatorial beta plane. *Journal of the Atmospheric Sciences*, *57*(13), 2169–2187.
- Xie, S., Cederwall, R., & Zhang, M. (2004). Developing long-term single-column model/cloud system-resolving model forcing data using numerical weather prediction products constrained by surface and top of the atmosphere observations. *Journal of Geophysical Research*, *109*, D01104. <https://doi.org/10.1029/2003JD004045>
- Xie, S., Lin, W., Rasch, P. J., Ma, P. L., Neale, R., Larson, V. E., et al. (2018). Understanding cloud and convective characteristics in version 1 of the E3SM atmosphere model. *Journal of Advances in Modeling Earth Systems*, *10*, 2618–2644. <https://doi.org/10.1029/2018MS001350>

- Xie, S., Wang, Y. C., Lin, W., Ma, H. Y., Tang, Q., Tang, S., et al. (2019). Improved diurnal cycle of precipitation in E3SM with a revised convective triggering function. *Journal of Advances in Modeling Earth Systems*, *11*, 2290–2310. <https://doi.org/10.1029/2019MS001702>
- Xie, S., Xu, K. M., Cederwall, R. T., Bechtold, P., Genio, A. D. D., Klein, S. A., et al. (2002). Intercomparison and evaluation of cumulus parametrizations under summertime midlatitude continental conditions. *Quarterly Journal of the Royal Meteorological Society*, *128*(582), 1095–1135. <https://doi.org/10.1256/003590002320373229>
- Xie, S., & Zhang, M. (2000). Impact of the convection triggering function on single-column model simulations. *Journal of Geophysical Research*, *105*(D11), 14,983. <https://doi.org/10.1029/2000JD900170>
- Xie, S., Zhang, M., Branson, M., Cederwall, R. T., Del Genio, A. D., Eitzen, Z. A., et al. (2005). Simulations of midlatitude frontal clouds by single-column and cloud-resolving models during the Atmospheric Radiation Measurement March 2000 cloud intensive operational period. *J. Geophys. Res.*, *110*, D15S03. <https://doi.org/10.1029/2004JD005119>
- Xie, S., Zhang, M., Boyle, J. S., Cederwall, R. T., Potter, G. L., & Lin, W. (2004). Impact of a revised convective triggering mechanism on community atmosphere model, version 2, simulations: Results from short-range weather forecasts. *Journal of Geophysical Research*, *109*, D14102. <https://doi.org/10.1029/2004JD004692>
- Xie, S., Zhang, Y., Giangrande, S. E., Jensen, M. P., McCoy, R., & Zhang, M. (2014). Interactions between cumulus convection and its environment as revealed by the MC3E sounding array. *Journal of Geophysical Research: Atmospheres*, *119*, 11,784–11,808. <https://doi.org/10.1002/2014JD022011>
- Xu, K. M., Zhang, M., Eitzen, Z. A., Ghan, S. J., Klein, S. A., Wu, X., et al. (2005). Modeling springtime shallow frontal clouds with cloud-resolving and single-column models. *Journal of Geophysical Research*, *110*, D15S04. <https://doi.org/10.1029/2004JD005153>
- Zhang, G. J. (2002). Convective quasi-equilibrium in midlatitude continental environment and its effect on convective parameterization. *Journal of Geophysical Research*, *107*(14), 4220. <https://doi.org/10.1029/2001JD001005>
- Zhang, G. J. (2003). Roles of tropospheric and boundary layer forcing in the diurnal cycle of convection in the U.S. Southern Great Plains. *Geophysical Research Letters*, *30*(24), 2281. <https://doi.org/10.1029/2003GL018554>
- Zhang, G. J., & Mcfarlane, N. A. (1995). Sensitivity of climate simulations to the parameterization of cumulus convection in the Canadian climate centre general circulation model. *Atmosphere-Ocean*, *33*(3), 407–446.
- Zhang, M., & Lin, J. (1997). Constrained variational analysis of sounding data based on column-integrated budgets of mass, heat, moisture, and momentum: Approach and application to. *Journal of the Atmospheric Sciences*, *54*, 1503–1524. Retrieved from [http://journals.ametsoc.org/doi/abs/10.1175/1520-0469\(1997\)054<1503:CVAOSD>2.0.CO;2](http://journals.ametsoc.org/doi/abs/10.1175/1520-0469(1997)054<1503:CVAOSD>2.0.CO;2)
- Zhang, M., Lin, J., Cederwall, R., Yio, J. J., & Xie, S. (2001). Objective analysis of ARM IOP data: Method and sensitivity. *Monthly Weather Review*, *129*, 295–311. Retrieved from. [http://journals.ametsoc.org/doi/abs/10.1175/1520-0493\(2001\)129<0295:OAOAID>2.0.CO;2](http://journals.ametsoc.org/doi/abs/10.1175/1520-0493(2001)129<0295:OAOAID>2.0.CO;2)
- Zhang, Y., & Klein, S. A. (2010). Mechanisms affecting the transition from shallow to deep convection over land: Inferences from observations of the diurnal cycle collected at the ARM Southern Great Plains site. *Journal of the Atmospheric Sciences*, *67*(9), 2943–2959. <https://doi.org/10.1175/2010JAS3366.1>
- Zhang, Y., Xie, S., Lin, W., Klein, S. A., Zelinka, M., Ma, P.-L., et al. (2019). Evaluation of clouds in version 1 of the E3SM atmosphere model with satellite simulators. *Journal of Advances in Modeling Earth Systems*, *11*, 1253–1268. <https://doi.org/10.1029/2018MS001562>
- Zheng, X., Golaz, J. C., Xie, S., Tang, Q., Lin, W., Zhang, M., et al. (2019). The summertime precipitation bias in E3SM Atmosphere Model Version 1 over the Central United States. *Journal of Geophysical Research: Atmospheres*, *124*, 8935–8952. <https://doi.org/10.1029/2019JD030662>